Hindawi
Shock and Vibration
Volume 2020, Article ID 8885546, 11 pages
https://doi.org/10.1155/2020/8885546

Research Article

Vibration Test and Shock Absorption of Coal Crusher Chambers in Thermal Power Plants (II): Numerical Analysis

Hanquan Yuan,[1] **Lihua Zhu**,[1,2] **Haoyi Zhou**,[1] **Dong Jiang**,[3] **Baoquan Liu**,[3] **Chunzhu Fan**,[3] **and Liujiu Tang**[3]

[1]*School of Civil Engineering, Xi'an University of Architecture & Technology, 13 Yanta Road, Xi'an 710055, China*
[2]*Key Lab of Structural Engineering and Earthquake Resistance, Ministry of Education (XAUAT), Xi'an 710055, China*
[3]*Northwest Electric Power Design Institute of China Power Engineering Consulting Group, Xi'an 710075, China*

Correspondence should be addressed to Lihua Zhu; zhulihuaxa@163.com

Received 21 July 2020; Revised 31 August 2020; Accepted 7 September 2020; Published 15 September 2020

Academic Editor: Ömer Cívalek

The coal crusher generates large vibrations when crushing coal blocks, which can affect the equipment itself, as well as the safety of the structure. In order to study the dynamic characteristics of coal crusher, a finite element model of the coal crusher chamber in the Shangluo power plant was built by using ABAQUS. Firstly, modal and harmonic response analyses were conducted, and the comparison shows that the numerical results are basically in accordance with the test results. Then, shock absorption research was performed using a parametric analysis that included the stiffness and position of the spring vibration isolator, the mass, and material of the vibration-isolation platform. Finally, the dynamic coefficient of a coal crusher was discussed. The results showed that, compared with the stiffness of the spring vibration isolator, the mass of the vibration-isolation platform had more influence on the vibration displacement of the coal crusher. To achieve better vibration isolation, the concrete platform is suggested, and the eccentricity of the spring vibration isolator should not exceed 5%. When static design method is adopted to calculate the bearing capacity of the supporting structure subjected to the dynamic load of the coal crusher, the dynamic coefficient of a coal crusher is suggested as 1.5.

1. Introduction

Compared with other industrial plants, the vibration source in a coal crusher chamber is more complex, and the vibration mechanism of the dynamic machine in the coal crusher chamber is still not very clear. Because of the lack of a relevant theoretical basis, designers can only learn from the research results of other similar dynamic machines in both the design stage and the later reinforcement stage.

Theoretically, vibration-isolation technology can effectively reduce the vibration of dynamic machines [1, 2]. It has been found that the vibration of the floor of a coal crusher chamber can be controlled by adopting this kind of technology, but the vibration displacements of coal crushers are very large. The current codes and specifications [3, 4] only limit the vibration displacements at the top surfaces of dynamic machine foundations, whereas those of the machine bodies are not specified. If the vibration displacement of a machine is too large, the machine may be subjected to rigid damage, which will reduce its reliability and service life.

Finite element method is a very timely and effective meshing method. This method has been widely used for analysis. In this study, a finite element model of a coal crusher chamber is established based on the data obtained in coal crusher chamber tests. This article consists of four sections, the dimensions of coal crusher chamber introduced in Section 2. Then, modal and harmonic response analyses of coal crusher chamber are analyzed by the finite element method. Section 3further discusses the vibration reduction parameters of coal crusher. Finally, some conclusions are listed in Section 4.

2. Finite Element Analysis

2.1. Modeling. The coal crusher chamber in the Shangluo power plant was used as the prototype for the developed finite element model. A three-dimensional finite element model of a coal crusher system and coal crusher chamber was built using ABAQUS [5, 6].

Beam elements were used for the frame, and shell elements were used for the floor slabs. Solid elements were used to simulate the coal crusher, hydraulic coupler, motor, and steel vibration-isolation platform. Springs and dashpots elements were used for the spring vibration isolators. Based on the actual structure, rigid connections were used for equipment-equipment connections and equipment-platform connections, whereas the platform and coal crusher chamber were connected by spring vibration isolators. In the coordinate system of the model, X represented the transverse direction of the coal crusher chamber, Y represented the longitudinal direction, and Z represented the vertical direction.

The mesh size of the finite element model was 100–200 mm. The finite element model is shown in Figure 1. Because of the simplification of the model, equivalent densities were adopted for the equipment and platform to keep their quality consistent with reality. The primary parameters of the equipment and platform are listed in Table 1. The primary parameters of the spring vibration isolators are listed in Table 2. The disturbing forces of the coal crusher system are listed in Table 3, and the action positions are shown in Figure 2.

2.2. Modal Analysis. A modal analysis was performed using the Block Lanczos method [7]. The first three structural modes are shown in Figure 3, and the natural frequencies of the structure found in the numerical results and test results are listed in Table 4.

As can be observed in Table 4, the numerical results are close to the test results, and the maximum error is not greater than 5%, which indicates that the model is reasonable and can be used for further calculations and analyses.

2.3. Harmonic Response Analysis. A harmonic analysis of a coal crusher under the service load was performed. The numerical results were then compared with the test results. The locations of the displacement measurement points on the coal crusher and platform are shown in Figure 4. The vibration amplitude–frequency curves from 0 to 20 Hz were obtained through a harmonic response analysis, which included the working speed of the coal crusher and motor. The typical amplitude–frequency curves under various working conditions are shown in Figure 5.

The vibration displacements of each point under each working condition, corresponding to the excitation frequency of 12.38 Hz, could be obtained from the amplitude–frequency curves. The square root of the sum of the squares (SRSS) method [8, 9] was used to process the data, which are listed in Table 5 (FS represents the displacement measurement points on the second floor slab, which correspond with those used in the vibration test).

Table 6 lists the numerical and test results for the maximum horizontal and vertical vibration displacements of the coal crusher body, platform, and second floor slab. The numerical results generally agree with the test results in terms of their orders of magnitude and variation tendencies, which verifies the accuracy of the finite element model and harmonic analysis.

2.4. Vibration-Isolation Efficiency. According to the Chinese Code [10], the single-degree-of-freedom model is used to design the vibration isolation of the coal crusher. In this model, the vibration-isolation efficiency was calculated by the frequency of the disturbing forces and the vibration-isolation system. The vibration displacements, velocities, and accelerations after vibration isolation are not involved in the calculation method of vibration-isolation efficiency. In the field test, the vibration-isolation efficiency was calculated by the dynamic response before and after vibration isolation. The spring vibration-isolation system was considered as a two-degree-of-freedom model in this calculation method. Both of these models are very different from a practical multi-degree-of-freedom model [11]. In order to study the differences between these three models, the numerical vibration-isolation efficiency of the spring vibration-isolation system was calculated and compared with the designed and measured vibration-isolation efficiencies.

When there are multiple disturbing forces, the transmissibility (TR) of a spring vibration-isolation system [12] can be calculated using the SRSS method, where the vibration-isolation efficiency is found as follows:

$$\eta = 1 - \mathrm{TR} = 1 - \sqrt{\frac{\sum F_i^2}{\sum P_i^2}}, \tag{1}$$

where F_i is the reaction force of the spring vibration isolators under working condition i and P_i is the disturbing force of working condition i.

The layout of the spring vibration isolators is shown in Figure 6. The numerical vibration-isolation efficiencies based on (1) are listed in Table 7.

The results showed that the numerical vibration-isolation efficiency of the spring vibration-isolation system was 87.09%, which was slightly lower than the designed vibration-isolation efficiency of 90%, indicating that the single-degree-of-freedom model was effective in the design of the spring vibration-isolation system. The measured vibration-isolation efficiency was 73.59%, which was lower than the previous two values. This may have been related to the installation, aging, and other factors of the spring vibration isolators.

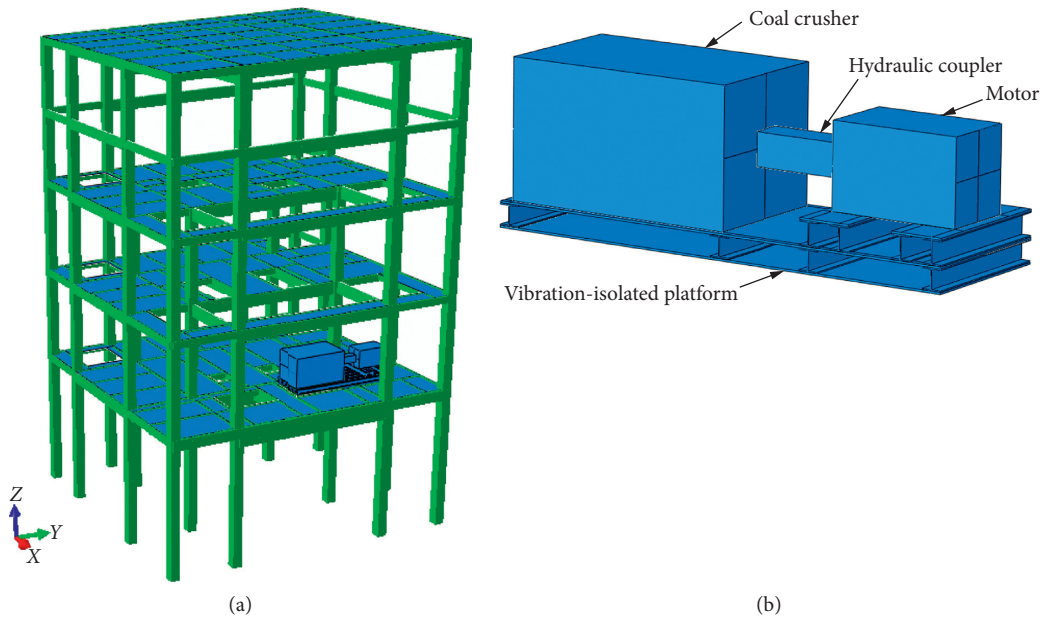

Figure 1: Finite element model. (a) Structure of coal crusher chamber. (b) Coal crusher system and vibration-isolation platform.

Table 1: Parameters of equipment and platform.

Parts		Size (mm)	Number	Weight (kg)	Equivalent density (kg/m^3)
Coal crusher		3585 × 2200 × 2100	1	23500	1418
Motor		2000 × 1200 × 1300	1	9200	2950
Hydraulic coupler		1500 × 500 × 500	1	1166	3100
Vibration-isolation platform	Steel plate 1	7385 × 2400 × 30	2	8000	5447
	Steel plate 2	800 × 2400 × 30	2		
	I-beam 1	330 × 300 × 10	4		
	I-beam 2	370 × 300 × 10	4		

Table 2: Parameters of spring vibration isolator.

Vertical stiffness of the vibration isolator (kN/m)	1150
Horizontal stiffness of the vibration isolator (kN/m)	897
Vertical damping factor (kN·s/m)	9.8
Horizontal damping factor (kN·s/m)	9.8
Damping ratio of the structure	0.05

Table 3: Disturbing forces of coal crusher system.

Equipment	Location	Direction		
		X (kN)	Y (kN)	Z (kN)
Coal crusher	$D1$	9	4.5	9
	$D2$	9	4.5	9
Motor	$D3$	2	1	2
	$D4$	2	1	2

3. Parametric Analysis of the Vibration Reduction of Coal Crusher

3.1. Stiffness of Spring Vibration Isolators and Mass of Vibration-Isolation Platform. As reported in the previous paper in this series, the vibration displacement of the coal crusher body could be reduced by controlling the vibration displacement of the platform. In order to study the influences of the stiffness [13] of the spring vibration isolators and the mass of the vibration-isolation platform on its vibration, these two parameters were changed; finite element models at vibration-isolation efficiencies of 60%, 70%, 80%, and 90% were obtained; and a harmonic response analysis was performed.

According to the Chinese code [10] for the vibration-isolation design of an auxiliary machine foundation in a thermal power plant, the design formulas for a spring vibration-isolation system are as follows:

$$K_z = \frac{\omega^2 M}{1 + (1/\eta)}, \tag{2}$$

$$C_z = 2\xi_z \sqrt{K_z m}, \tag{3}$$

where ω is the circular frequency of the disturbing force; and K_z, M, C_z, and ξ_z are the vertical stiffness, mass, vertical damping coefficient, and vertical damping ratio of the spring vibration-isolation system, respectively.

The parameters of the spring vibration-isolation system under each isolation efficiency could be obtained using

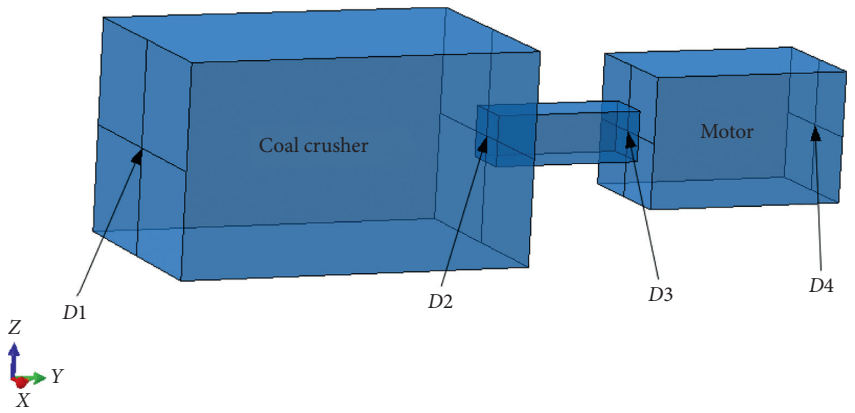

Figure 2: Positions of the disturbing forces.

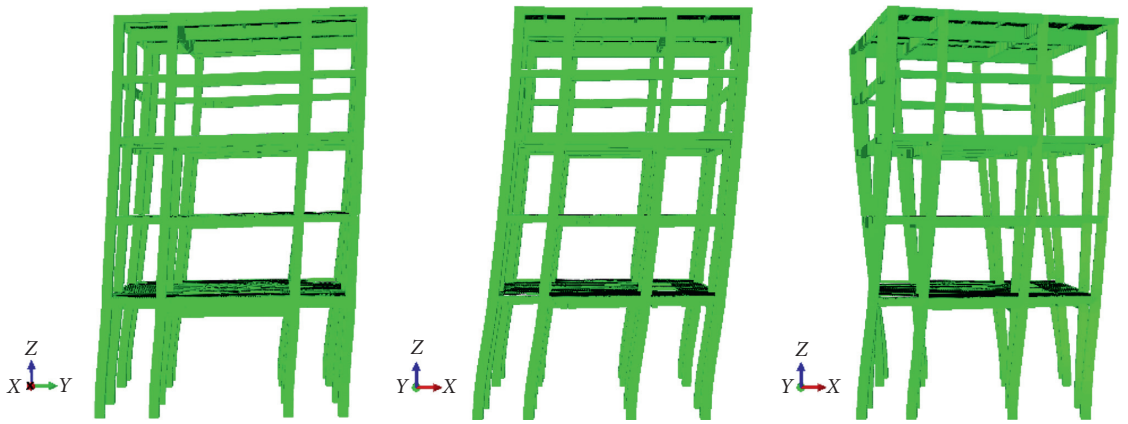

Figure 3: First three modes of the structure. (a) First modal shape, (b) second modal shape, and (c) third modal shape.

Table 4: Natural frequencies of structure from numerical results and test results.

Order	Calculation frequency (Hz)	Test frequency (Hz)	Vibration modal shape	Error
1	1.020	0.987	Y direction horizontal vibration	3.24%
2	1.052	1.012	X direction horizontal vibration	3.80%
3	1.211	—	Z direction rotational vibration	—
4	2.887	2.763	Y direction horizontal vibration	4.30%
5	2.895	2.788	X direction horizontal vibration	3.70%
6	3.626	—	Z direction rotational vibration	—

formulas (2) and (3). In these calculations, $\xi_z = 0.1$; the horizontal stiffness of the system was 0.78 times the vertical stiffness; and the horizontal damping coefficient was the same as the vertical damping coefficient [14]. The parameters of the spring vibration-isolation system under each vibration-isolation efficiency are listed in Table 8.

The discussion in this section is based on the values obtained at displacement measurement point PT4, as shown in Figure 4. The vibration displacements at PT4, corresponding to each model, are shown in Figure 7.

It can be observed that when the mass of the vibration-isolation platform remained unchanged, but the stiffness of the spring vibration isolators was decreased, the vibration-isolation efficiency of the spring vibration-isolation system increased from 60% to 90%, the horizontal vibration displacement of the platform decreased from 215.01 μm to 117.01 μm, and the vertical vibration displacement decreased from 217.15 μm to 119.10 μm. When the stiffness of the spring vibration isolators remained unchanged, but the mass of the vibration-isolation platform was increased, the vibration-isolation efficiency of the spring vibration-isolation system increased from 60% to 90%, the horizontal vibration displacement of the platform decreased from 226.13 μm to 89.10 μm, and the vertical vibration displacement decreased

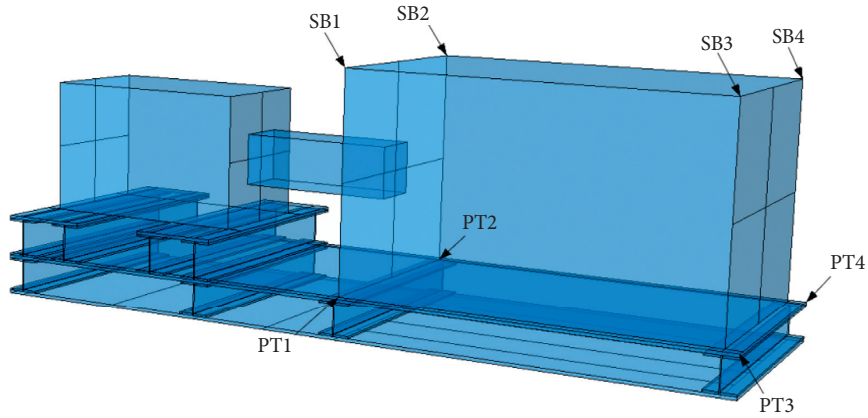

Figure 4: Locations of displacement measurement points.

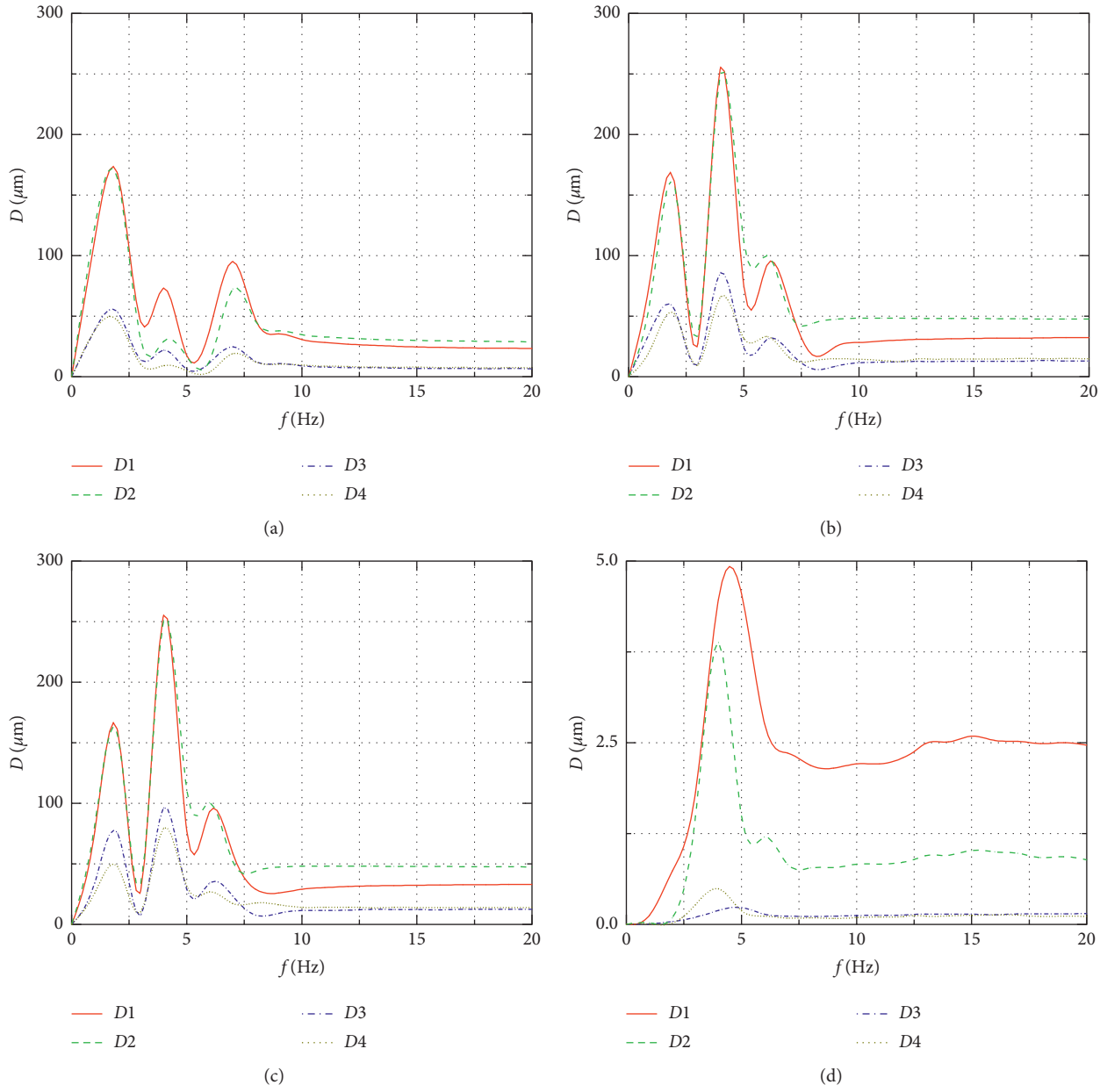

Figure 5: Typical displacement–frequency curves: (a) PT1X, (b) PT1Z, (c) SB1Z, and (d) FS1Z.

Table 5: Vibration displacements at points on coal crusher and platform.

Location	Direction		
	X (μm)	Y (μm)	Z (μm)
SB1	60.2	29.74	60.5
SB2	60.2	81.5	42.32
SB3	124.31	29.74	126.78
SB4	124.31	81.5	119.39
FS	0.25	0.27	2.51
PT1	42.39	38.53	61.08
PT2	42.4	32.23	41.15
PT3	117.01	38.59	127.18
PT4	117.01	31.68	119.1

Table 6: Vibration displacements from numerical results and test results.

Location	Direction	Numerical results (μm)	Test results (μm)
Coal crusher	X	124.31	149.09
	Y	81.5	56.77
	Z	126.78	164.75
Vibration-isolated platform	X	117.01	154.09
	Y	38.59	130.93
	Z	127.18	138.34
Second floor	X	0.25	2.44
	Y	0.27	1.96
	Z	2.51	2.75

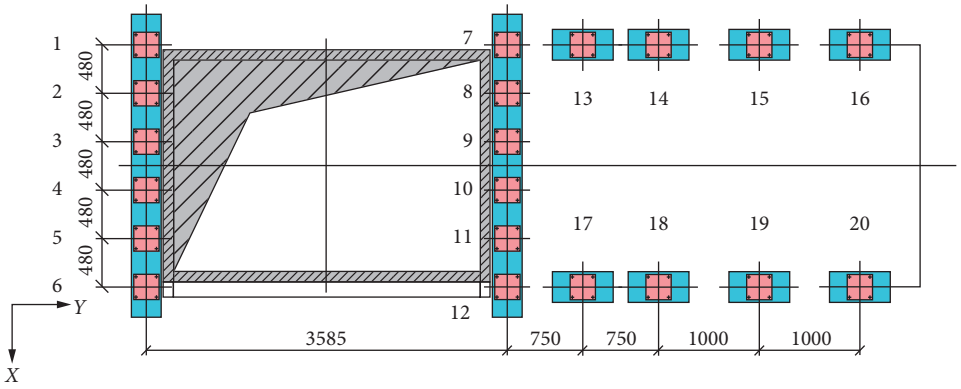

Figure 6: Positions of spring vibration isolators.

from 270.17 μm to 92.65 μm. Therefore, decreasing the stiffness of the spring vibration isolators and increasing the mass of the vibration-isolation platform could improve the vibration-isolation efficiency of the spring vibration-isolation system. Thus, the vibration displacement of the vibration-isolation platform could be reduced.

In order to compare the influences of these two parameters on the vibration displacement of the platform, the vibration displacement of the point at a 70% vibration-isolation efficiency was regarded as the reference value, and the ratio of the maximum vibration displacement of the point at each vibration-isolation efficiency to the reference value was calculated, with the results listed in Table 9.

The results showed that, for the vibration-isolation platform, the variations in the horizontal vibration displacement and vertical vibration displacement were basically the same even if the stiffness of the spring vibration isolators was decreased or the mass of the vibration-isolation platform was increased. Regardless of the vibration displacement of the vibration-isolation platform in the horizontal or vertical direction, the influence of the mass of the vibration-isolation platform was obviously greater than that of the stiffness of the spring vibration isolators. Therefore, the

Table 7: Calculated vibration-isolation efficiencies.

Spring vibration isolators	Reaction force (kN)			
	Condition *D*1	Condition *D*2	Condition *D*3	Condition *D*4
1	0.121	0.042	0.003	0.013
2	0.121	0.039	0.003	0.014
3	0.120	0.036	0.003	0.015
4	0.095	0.032	0.004	0.017
5	0.118	0.029	0.005	0.018
6	0.117	0.025	0.006	0.019
7	0.043	0.053	0.013	0.017
8	0.042	0.049	0.012	0.016
9	0.041	0.046	0.011	0.015
10	0.040	0.043	0.010	0.013
11	0.039	0.039	0.009	0.012
12	0.039	0.036	0.008	0.011
13	0.026	0.055	0.015	0.022
14	0.070	0.057	0.017	0.026
15	0.043	0.060	0.020	0.032
16	0.065	0.063	0.023	0.038
17	0.089	0.038	0.010	0.015
18	0.024	0.040	0.012	0.020
19	0.047	0.043	0.015	0.026
20	0.069	0.046	0.018	0.032
Total of the reaction force	1.37	0.87	0.22	0.39
Disturbing force	9	9	2	2
Vibration-isolation efficiency	87.09%			

Table 8: Parameters of spring vibration-isolation system under each vibration-isolation efficiency.

Varying parameter	Parameters of the isolators	Vibration-isolation efficiency			
		90%	80%	70%	60%
Stiffness of spring vibration isolators	Vertical stiffness (kN/m)	1150	2109	2920	3616
	Horizontal stiffness (kN/m)	897	1645	2278	2820
	Vertical damping factor (kN·s/m)	9.8	13.3	15.6	17.4
	Horizontal damping factor (kN·s/m)	9.8	13.3	15.6	17.4
	Mass of vibration-isolation platform (t)	8			
Mass of vibration-isolated platform	Vertical stiffness (kN/m)	2920			
	Horizontal stiffness (kN/m)	2278			
	Vertical damping factor (kN·s/m)	24.9	18.4	15.6	14.1
	Horizontal damping factor (kN·s/m)	24.9	18.4	15.6	14.1
	Mass of vibration-isolation platform (t)	72.4	24.1	8	0

method of increasing the mass of the vibration-isolation platform has a better vibration reduction effect.

3.2. Positions of Spring Vibration Isolators. In order to study the influence of an eccentric arrangement of spring vibration isolators on the vibration of the coal crusher, their positions were changed, and the vibration displacements of the coal crusher were then compared with the original results.

Eccentricity refers to the relative error between the center of the spring vibration isolator's rigidity and the center of mass of the vibration-isolation platform. Its calculation formula is as follows:

$$\Delta X = \left| \frac{X_k - X_m}{L_X} \right|, \quad (4)$$

where $\triangle X$ is the eccentricity in direction X; X_k is the center of rigidity of the spring vibration isolator in the X direction; X_m is the center of mass of the vibration-isolation platform in the X direction; and L_X is the length of the vibration-isolation platform in the X direction.

The position of spring vibration isolator No. 1 was used as the coordinate origin to establish a rectangular coordinate system. The corresponding coordinates of each spring vibration isolator are listed in Table 10. The maximum vibration displacements in all directions on the machine were determined and compared with the calculated results for the original model, as listed in Table 11.

The results showed that when the eccentricity was 5%, the horizontal displacement of the machine increased by 15%, and the vertical displacement increased by 22.42%; when the eccentricity was 10%, the horizontal displacement

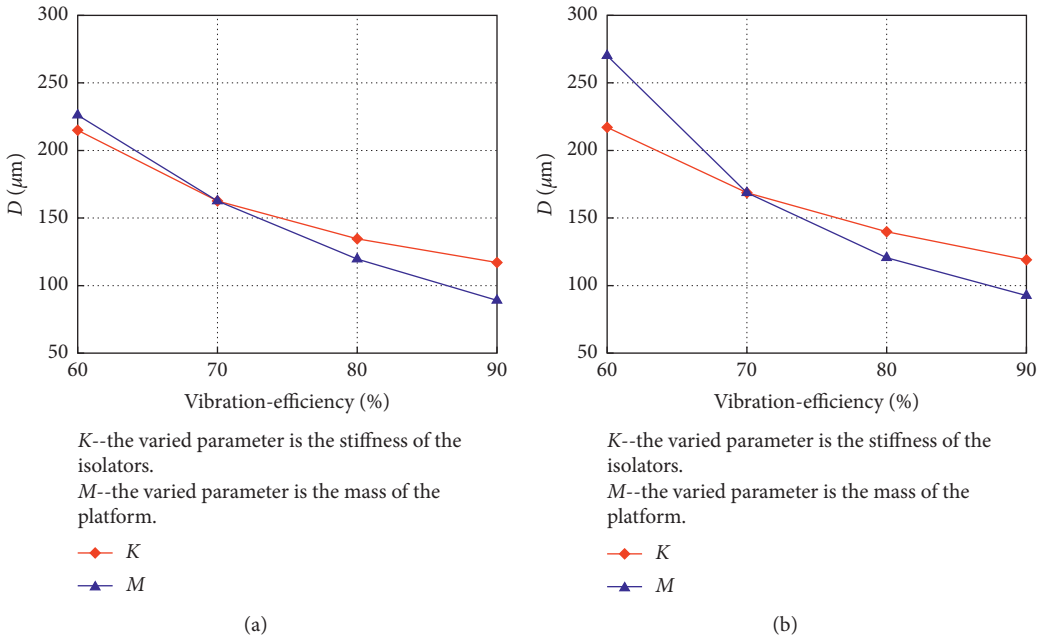

Figure 7: Vibration displacements of each point under each vibration-isolation efficiency. (a) PT4X and (b) PT4Z.

Table 9: Ratio of vibration displacement of point to reference value at each vibration-isolation efficiency.

Varying parameter	Direction	Vibration-isolation efficiency			
		90%	80%	70%	60%
Stiffness of spring vibration isolators	X	0.72	0.83	1	1.32
	Z	0.71	0.83	1	1.29
Mass of vibration-isolation platform	X	0.55	0.74	1	1.39
	Z	0.55	0.71	1	1.6

of the machine increased by 52%, and the vertical displacement increased by 50.56%. The vibration displacement of the machine increased with the eccentricity but varied greatly. Considering machine operation safety, it is suggested that the eccentricity should not exceed 5%.

3.3. Comparison of Steel Platform and Concrete Platform. At present, steel platforms are widely used by equipment manufacturers in vibration-isolation design, while concrete platforms are adopted by design institutes. Compared with a concrete platform, a steel platform is lighter in mass and smaller in volume. To study the differences between steel and concrete platforms, a concrete platform finite element model was established. Then, the numerical results derived from the harmonic response analysis were compared with the numerical results for a steel platform reported in Section 2.3.

Based on the "*Design Code of Vibration Isolation of Auxiliary Machine Foundation in Fossil Fuel Power Plant*" (DL/T 5188-2004) [10], the following parameters were used for the concrete platform modeled in this study. The thickness was 1 m, the cross-sectional dimensions in the vertical direction were 7085 mm × 2400 mm, and the total mass was 47.31 t. The parameters of the spring vibration isolators at an vibration-isolation efficiency of 90% were calculated using formula (2) and are listed in Table 12. The finite element model of the concrete platform is shown in Figure 8. The maximum vibration displacements of the steel and concrete platforms are listed in Table 13.

Based on the "*Technical Code for the Design of Civil Structure of Fossil-Fired Power Plant*" (DL 5022-2012) [4], the limit values of the vibration displacements of the vibration-isolation platform for a coal crusher are 0.15 mm in the vertical direction and 0.20 mm in the horizontal direction.

The analysis results showed that as long as the steel and concrete platforms were designed in accordance with the code requirements, the vibration displacements of both could meet the code requirements. When the concrete platform was adopted, the displacements in all directions of the vibration-isolation platform were lower than those when a steel platform was adopted. Therefore, it is suggested that concrete platforms be adopted in the vibration-isolation design of coal crushers.

3.4. Dynamic Coefficients of Coal Crushers. A dynamic coefficient [3] refers to a coefficient adopted in the static design of a structure or component under dynamic loads, and its value is the ratio of the maximum dynamic response of the structure or component to the corresponding static

Table 10: Positions of spring vibration isolators in model.

Spring vibration isolators	Original model		The model with an eccentricity of 5%		The model with an eccentricity of 10%	
	X	Y	X	Y	X	Y
1	0	0	0	0	0	0
2	0.48	0	0	0	0	0
3	0.96	0	0.48	0	0.48	0
4	1.44	0	0.96	0	0.96	0
5	1.92	0	1.44	0	1.44	0
6	2.4	0	1.92	0	1.92	0
7	0	3.585	0	3.585	0	3.585
8	0.48	3.585	0.48	3.585	0	3.585
9	0.96	3.585	0.96	3.585	0.48	3.585
10	1.44	3.585	1.44	3.585	0.96	3.585
11	1.92	3.585	1.92	3.585	1.44	3.585
12	2.4	3.585	2.4	3.585	1.92	3.585
13	0	4.335	0	4.335	0	4.335
14	0	5.085	0	5.085	0	5.085
15	0	6.085	0	6.085	0	6.085
16	0	7.085	0	7.085	0	7.085
17	2.4	4.335	2.4	4.335	2.4	4.335
18	2.4	5.085	2.4	5.085	2.4	5.085
19	2.4	6.085	2.4	6.085	2.4	6.085
20	2.4	7.085	2.4	7.085	2.4	7.085
Center of rigidity	1.2	—	1.08	—	0.96	—
Center of mass	1.2	—	1.2	—	1.2	—
Relative error	0%	—	5%	—	10%	—

Table 11: Influence of eccentric positions of spring vibration isolators.

Location	Type	5%			10%		
		X (μm)	Y (μm)	Z (μm)	X (μm)	Y (μm)	Z (μm)
Coal crusher	Before eccentricity	124.31	81.5	126.78	124.31	81.5	126.78
	After eccentricity	136.74	93.72	155.21	188.95	95.97	190.88
	Change rate	10.00%	15.00%	22.42%	52.00%	17.75%	50.56%

Table 12: Parameters of spring vibration isolators for concrete platform.

Vertical stiffness of the vibration isolator (kN/m)	2200
Horizontal stiffness of the vibration isolator (kN/m)	1716
Vertical damping factor (kN·s/m)	50
Horizontal damping factor (kN·s/m)	50

response. The values for the dynamic coefficients of coal crushers with vibration-isolation systems are not specified in the current specifications. Therefore, this study calculated the dynamic coefficients of the finite element models established in Section 3.1.

The vibration displacements at the bottom of the spring vibration isolators (i.e., the support beams) were used to calculate the dynamic coefficients. Static vibration displacements were obtained by applying static forces equal to the disturbing forces after vibration isolation at the same position, where the finite element model was the same as that previously discussed. Table 14 lists the calculation results for the dynamic coefficients of displacement measurement points $L1$–$L12$ (see Figure 6) under each vibration-isolation efficiency.

The results showed that the maximum values of the dynamic coefficients under the different vibration-isolation efficiencies were generally equal to 1.3. Theoretically, the dynamic coefficient is related to the frequency of the structure and machine; it has basically no relationship with the vibration-isolation efficiency. Based on Table 10, it is recommended that a value of 1.5 be used for the dynamic coefficient of a coal crusher.

The design value of the disturbing force generated by the machine should be used to calculate the dynamic internal force of the support structure. The calculation formula is as follows [15]:

$$P_e = K_d \times P, \tag{5}$$

where P_e is the design value of the disturbing force; P is the standard value of the disturbing force; and K_d is the

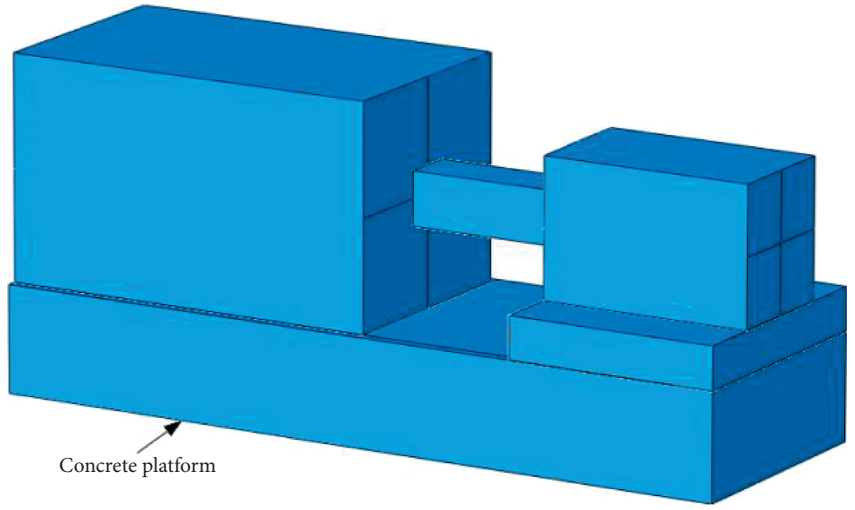

Figure 8: Concrete vibration-isolation platform.

Table 13: Comparison of vibration displacements between the steel platform and concrete platform.

Location	Material of platform	Direction		
		X (μm)	Y (μm)	Z (μm)
Coal crusher	Steel	124.31	81.5	126.78
	Concrete	100.8	53.62	78.89
Vibration-isolation platform	Steel	117.01	38.59	127.18
	Concrete	72.56	26.98	80.19

Table 14: Dynamic coefficients of points under each vibration-isolation efficiency.

Location	Dynamic displacement (μm)				Static displacement (μm)				Dynamic coefficients			
	90%	80%	70%	60%	90%	80%	70%	60%	90%	80%	70%	60%
$L1$	2.37	4.67	6.88	9.01	1.78	3.57	5.35	7.14	1.33	1.31	1.29	1.26
$L2$	1.09	2.15	3.14	4.09	1.08	2.15	3.23	4.31	1.01	1.00	0.97	0.95
$L3$	2.47	4.88	7.20	9.48	1.97	3.94	5.92	7.89	1.25	1.24	1.22	1.20
$L4$	1.13	2.22	3.27	4.30	1.21	2.42	3.63	4.84	0.93	0.92	0.90	0.89
$L5$	1.15	2.27	3.36	4.45	1.31	2.61	3.92	5.23	0.88	0.87	0.86	0.85
$L6$	1.15	2.27	3.38	4.53	1.36	2.72	4.08	5.44	0.85	0.83	0.83	0.83
$L7$	1.12	2.23	3.33	4.50	1.36	2.73	4.09	5.45	0.82	0.82	0.81	0.83
$L8$	1.07	2.13	3.20	4.35	1.32	2.63	3.95	5.26	0.81	0.81	0.81	0.83
$L9$	2.39	4.74	7.09	9.49	2.14	4.27	6.41	8.54	1.12	1.11	1.11	1.11
$L10$	2.49	4.94	7.36	9.83	2.21	4.41	6.61	8.81	1.13	1.12	1.12	1.12
$L11$	2.55	5.03	7.48	9.93	2.19	4.38	6.57	8.76	1.16	1.15	1.14	1.13
$L12$	2.54	5.00	7.41	9.80	2.11	4.22	6.34	8.45	1.20	1.18	1.17	1.16

dynamic overload coefficient, where the value for a rotary machine is four.

Thus, the static design method could be adopted to calculate the bearing capacity of the support structure subjected to the dynamic load of the coal crusher, and the suggested value for the static load is the sum of the self-weight of the machine, platform, and six times the disturbing force.

4. Conclusion

This study investigated methods for reducing the vibration of a coal crusher in a thermal power plant using finite element analyses. The major conclusions are summarized as follows:

(1) The finite element analysis results were shown to be basically consistent with the measured results, which verified that it was feasible to use the finite element method to analyze the vibration performance of a coal crusher.

(2) The dynamic characteristics and vibration displacements under the disturbing forces of the coal crusher chamber could be accurately estimated using modal and harmonic analyses. Thus, this method provided a basis for dynamically optimizing the design of the coal crusher chamber and vibration-isolated foundation of a coal crusher.

(3) The vibration-isolation efficiency of the multi-degree-of-freedom model was slightly less than the

designed value, which indicated that a vibration-isolation design based on a single-degree-of-freedom model could meet the accuracy requirements. The measured vibration-isolation efficiency was less than the previous two values, which may have been related to the installation, aging, and other factors of the spring vibration isolators.

(4) The results involving decreasing the stiffness of the spring vibration isolator and increasing the mass of the vibration-isolation platform could reduce the vibration displacement of the platform of the coal crusher, but the influence of the mass of the vibration-isolation platform was obviously greater than that of the stiffness of the spring vibration isolators. Therefore, it is suggested that the latter be adopted in the displacement optimization of a coal crusher.

(5) Both steel and concrete platforms could meet the design requirements, but, compared to the steel platform, the vibration displacements of the concrete platforms were smaller, and they had a better vibration-isolation effect. Considering the machine operation safety, it is suggested that the eccentricity of the spring vibration isolator should not exceed 5%.

(6) The static design method could be adopted to calculate the bearing capacity of the support structure subjected to the dynamic load of the coal crusher, and the dynamic coefficient of a coal crusher is suggested as 1.5.

Data Availability

The data used to support the findings of this study are available from the corresponding author upon request.

Conflicts of Interest

The authors declare that they have no conflicts of interest.

Acknowledgments

The present work was funded by the project of the Shaanxi Province Key Research and Development Program on Industry Innovation Chain (2018ZDCXL-SF-03-03-01).

References

[1] M. K. Kim, Y. S. Choun, and J. M. Seo, "Demonstration of the vibration control performance of coil spring-viscous damper systems by measuring the vibration of an emergency diesel generator," *Journal of Vibration and Control*, vol. 16, no. 2, pp. 207–229, 2010.

[2] J. Kumar and V. Boora, "Dynamic response of a machine foundation in combination with spring mounting base and rubber pad," *Journal of Geotechnical and Geoenvironmental Engineering*, vol. 27, no. 3, pp. 379–389, 2009.

[3] China Planning Press, *Code For Design of Dynamic Machine Foundation (GB50040-1996)*, China Planning Press, Beijing, China, 1997.

[4] China Planning Press, *Technical Code for the Design of Civil Structure of Fossil-Fired Power Plant (DL5022-2012)*, China Planning Press, Beijing, China, 2012.

[5] Springer International Publishing, *Troubleshooting Finite-Element Modeling with Abaqus*, Springer International Publishing, New York, NY, USA, 2019.

[6] E. Jiaqiang, G. Liu, T. Liu et al., "Harmonic response analysis of a large dish solar thermal power generation system with wind-induced vibration," *Solar Energy*, vol. 181, pp. 116–129, 2019.

[7] Y. Lu, P. Xiang, P. Dong, X. Zhang, and J. Zeng, "Analysis of the effects of vibration modes on fatigue damage in high-speed train bogie frames," *Engineering Failure Analysis*, vol. 89, pp. 222–241, 2018.

[8] E. Heredia-Zavoni, "The complete SRSS modal combination rule," *Earthquake Engineering & Structural Dynamics*, vol. 40, no. 11, pp. 1181–1196, 2011.

[9] D. M. Huang, L. D. Zhu, and W. Chen, "Covariance proper transformation-based pseudo excitation algorithm and simplified SRSS method for the response of high-rise building subject to wind-induced multi-excitation," *Engineering Structures*, vol. 100, pp. 425–441, 2015.

[10] China Electric Power Press, *Design Code of Vibration Isolation of Auxiliary Machine Foundation in Fossil Fuel Power Plant (DL/T5188-2004)*, China Electric Power Press, Beijing, China, 2004.

[11] I. Politopoulos and H. K. Pham, "Floor spectra of mixed base isolated structures," *Bulletin of Earthquake Engineering*, vol. 9, no. 4, pp. 1115–1135, 2011.

[12] Y. Q. Song, X. Q. Zhou, and Y. Fu, "Discussion on calculation method of vibration isolation efficiency for turbogenerator," *Engineering Journal of Wuhan University*, vol. 46, no. 1, pp. 220–224, 2013, in Chinese.

[13] X. Y. Lei and C. D. Jiang, "Analysis of vibration reduction effect of steel spring floating slab track with finite elements," *Journal of Vibration and Control*, vol. 22, no. 6, pp. 1462–1471, Article ID 1077546314539372, 2016.

[14] L. H. Zhu, J. Dai, and G. L. Bai, "Sensor placement optimization of vibration test on medium-speed mill," *Shock and Vibration*, vol. 2015, no. 8, 9 pages, Article ID 690196, 2015.

[15] China Planning Press, *Code For Design of Building and Structure of Coal Mine of Preparation Plant (GB50583-2010)*, China Planning Press, Beijing, China, 2010.